

Juha Heiskala, Kalle Kotilahti, and Ilkka Nissilä. 2005. An application of perturbation Monte Carlo in optical tomography. In: Proceedings of the 27th Annual International Conference of the IEEE Engineering in Medicine and Biology Society (IEEE-EMBS 2005). Shanghai, China. 1-4 September 2005, pages 274-277.

© 2005 IEEE

Reprinted with permission.

This material is posted here with permission of the IEEE. Such permission of the IEEE does not in any way imply IEEE endorsement of any of Helsinki University of Technology's products or services. Internal or personal use of this material is permitted. However, permission to reprint/republish this material for advertising or promotional purposes or for creating new collective works for resale or redistribution must be obtained from the IEEE by writing to pubs-permissions@ieee.org.

By choosing to view this document, you agree to all provisions of the copyright laws protecting it.

An application of perturbation Monte Carlo in optical tomography

Juha Heiskala, Kalle Kotilahti and Ilkka Nissilä

Abstract—Haemodynamic changes related to activation of the human visual cortex were studied using optical imaging. The change in oxyhaemoglobin concentration in the visual cortex was estimated using a perturbation Monte Carlo (pMC) method. Comparison to a topographic map obtained using the modified Beer-Lambert law and interpolation is given.

I. INTRODUCTION

Diffuse optical tomography is an emerging non-invasive medical imaging modality that uses near-infrared (NIR) light in the wavelength range between 700 and 900 nm. The method uses surface measurements of near-infrared light that has traveled through tissue. Strong scattering makes propagation of near-infrared light in most human tissues highly diffusive which makes the task of reconstructing the internal optical properties a complicated one.

Methods of interpreting optical imaging data are numerous, and they vary in accuracy and level of complexity. The choice of method depends on what information one wants to extract.

In near-infrared optical spectroscopy (NIRS), the goal is to estimate the changes in the concentrations of physiologically important chromophores in response to a stimulus or a physiological change. The magnitude of the changes can be estimated using the modified Beer-Lambert Law (MBLL) if certain assumptions are true. In the absence of a light-propagation model, the background optical properties are assumed to be homogeneous and the physiological change global. With this formalism, a localized change in the parameters in the tissue is generally reconstructed as a larger-volume change with lower contrast. This is due to the relatively low spatial resolution of the method.

In optical imaging, multiple light sources and detectors are used. Any change in the signal during experiment is generally assumed to be due to changes in optical properties either in the skin or in the underlying area of the brain.

In optical tomography, the aim is to solve for the spatial distribution of the optical properties or changes in them. This requires an explicit model of light propagation in the tissue and a method for the solution of the inverse problem (image reconstruction).

J. Heiskala is with the BioMag Laboratory, Helsinki University Central Hospital, P.O. Box 340, 00029 HUS Finland and Helsinki Brain Research Centre, P.O. Box 9, 00014 University of Helsinki, Helsinki, Finland Juha.Heiskala@iki.fi

K. Kotilahti is with the Laboratory of Biomedical Engineering, Helsinki University of Technology, P.O. Box 2200, 02015 HUT, Finland and Helsinki Brain Research Centre Kalle.Kotilahti@hut.fi

I. Nissilä is with the Athinoula A. Martinos Center for Biomedical Imaging, Massachusetts General Hospital, 149 13th St., Charlestown, MA 02129, USA inissila@nmr.mgh.harvard.edu

The propagation of near-infrared radiation in tissue can be modelled with a good accuracy by the radiative transfer equation (RTE). A direct solution to the RTE is a numerically complex problem which is currently studied by several groups.

Commonly used forward models include solving the diffusion approximation to the RTE, often with finite element methods (FEM) and Monte Carlo (MC) simulation, which is used to solve the RTE. MC methods are accurate given that a sufficient number of photon paths are calculated, and they are well suited for modeling light propagation in geometrically complex objects such as the human head [1]. Due to the large number of photons that need to be simulated to obtain accurate results, they are not applicable to unconstrained reconstruction of optical properties of tissues. However, often it is sufficient to study the changes in optical properties brought about by phenomena being studied, such as the hemodynamic changes due to activation of the brain. In this case, the magnitude of the optical property change is relatively small (<20%) and we can assume that the localized perturbation causes only small change in the photon paths, thus a linear reconstruction method is sufficient. These kinds of reconstruction problems can be handled by perturbation Monte Carlo (pMC) methods.

We present an optical tomography experiment involving activation in the human visual cortex. The changes in the concentration of oxyhaemoglobin in the head are estimated using pMC and the results are compared with an activation map generated using optical topography with the MBLL method.

II. METHODS

A. Brain activation imaging

1) *Experimental setup*: We used the frequency domain optical tomography instrument developed at Helsinki University of Technology [2] for studying haemodynamic responses in the brain during visual stimulation. The device has 16 parallel detector channels and 16 time-multiplexed source channels.

We applied an array of 18 optical fibers, of which 8 were sources and ten were detectors. The array was placed on the back of the subject's head over the visual cortex as shown in Figure 1. Two wavelengths (760 nm and 830 nm) were used. The image refresh rate was 0.5 Hz.

As stimulus, we used a reversing (8 Hz) checkerboard image that was shown to the subject on the screen of a laptop computer. The stimulus was shown for 5 s, followed by a 25 s pause. This sequence was repeated 18 times.

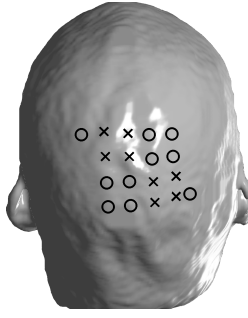


Fig. 1. The organization of optical source and detector fibers on the back of the subject's head. Crosses stand for sources, circles for detectors.



Fig. 2. A sagittal slice of the 3D anatomical model.

The locations of the optical fibers relative to three anatomical landmarks (nasion and the two preauricular points) on the head were measured using a Polhemus Fastrack[®] instrument [3]. This and anatomical MR imaging allowed us to determine the locations of the fibers relative to the subject's brain.

B. Modeling

1) *Monte Carlo simulation*: We studied the imaging situation with our Monte Carlo (MC) method which is capable of modeling light propagation in a complex tissue model [4].

In our MC implementation, the tissue is divided into volume elements (voxels), each of which may have different optical properties [1]. The optical properties of the model include absorption, anisotropic scattering, and the index of refraction. We obtained an anatomically accurate tissue model by segmenting a 3D MR image of the head of the subject into different tissue classes. A slice from the segmented head volume is shown in Figure 2. Since the locations of the optical fibers are known relative to known positions of the subject's head, they can also be accurately located in the tissue model.

In MC, an image of the light propagation is obtained by tracing the paths of individual photons or photon packets as they are scattered and absorbed within the tissue. The pathlength l of the photon between scattering events is drawn from an exponential distribution with probability distribution $\exp(-\mu_s l)$, where μ_s is the scattering coefficient of the tissue. The absorption is handled by reducing weight of the photon packet by $\exp(-\mu_a l)$ at each scattering event, where μ_a is the absorption coefficient. Good explanations of the rules of photon propagation exist in previous literature [5], [6], and we shall not go into detail here.

2) *Perturbation Monte Carlo*: The heavy computational burden of MC simulation prohibits its use for the iterative reconstruction of the optical properties of tissue without any prior knowledge. In the case of brain activation imaging, however, rather than trying to reconstruct the complete spatial distribution of optical properties, we only need to consider the changes in the optical properties. The tissue property distribution is assumed to be known, either based on the MR image of the subject, or based on a general head model, if an anatomical model of the subject is not available. Literature values for optical properties of different tissues can be used. The situation can be further simplified by assuming that the changes take place in specific tissues, and constraining the changes in optical properties to these tissues.

In pMC, information about the path of photon packets reaching specific detectors is accumulated. The effect of specific changes in optical properties of the tissue can be estimated by re-weighting these photon biographies. A perturbation in a region of the tissue being imaged changes the weight \hat{w} a photon packet contributes to the detected signal into [7], [8], [9]

$$\hat{w} = w \left(\frac{\hat{\mu}_s / \hat{\mu}_t}{\mu_s / \mu_t} \right)^j \left(\frac{\hat{\mu}_t}{\mu_t} \right)^j \exp[-(\hat{\mu}_t - \mu_t)L] \quad (1)$$

where $\hat{\mu}_s$ and $\hat{\mu}_a$ are the perturbed scattering and absorption coefficients and $\hat{\mu}_t = \hat{\mu}_s + \hat{\mu}_a$. j is the number of scattering events in the perturbed region, and L is the total pathlength in the perturbed region. Re-weighting photon biographies in this manner can be used for studying the effects of perturbations in both μ_a and μ_s . In our case, we assume the changes to occur only in μ_a . Assuming multiple perturbed regions with different changes in μ_a , the re-weighted contribution of a photon packet now becomes

$$\hat{w} = w \exp\left[-\sum_r (\hat{\mu}_a(r) - \mu_a(r))l_r\right] \quad (2)$$

Here the sum in the exponential function goes through all perturbed regions r . $\hat{\mu}_a(r)$ and $\mu_a(r)$ are the perturbed and unperturbed absorption coefficients in the region, and l_r is the path length traveled by the photon in the region.

The signal W_d at a detector is obtained as the sum of weights of photons that reach the detector. The derivatives $\partial W_d / \partial \mu_a$ can be obtained analytically from Eq. 2.

3) *Topographic mapping*: A topographic 2D image of the changes in haemodynamics may be obtained using the modified Beer-Lambert law which gives the change in signal intensity in response to changes in concentrations of absorbers as

$$A(\lambda) = A_0(\lambda) \exp\left[-d \cdot DPF \cdot \sum \Delta C_i \alpha_i(\lambda)\right] \quad (3)$$

where the sum in the exponential goes over different absorbers, C_i is the concentration of the i th absorber and α_i is the specific extinction coefficient of the absorber at wavelength λ . d is the distance between the source and the detector. DPF (Differential Pathlength Factor) is an experimentally determined scaling factor that gives the relation of the average pathlength traveled by a photon between a

source and a detector and the geometric distance. In optical topography, the change in absorption is generally assumed to depend mainly on changes in the concentrations of oxy- and deoxyhaemoglobin. Using two wavelengths, we get two equations from which concentrations of the two absorbers can be calculated.

For visualization, the change in absorption is assumed to be located at the midpoint of the line between the source and the detector. A map of the changes in oxy- and deoxyhaemoglobin is obtained by doing an interpolation.

C. Reconstruction of optical properties

We applied pMC to interpretation of our experimental data as well as a simulated case.

1) *Experiment*: The difference in experimental data recorded during activation and during resting state was calculated for each case. The resting state signal intensity was calculated as the average of the 5 s preceding the stimulus and the activated state signal intensity was taken at 5 s after the stimulus.

An MC simulation was carried out to produce the photon biographies. The contributions of photon packets were scaled such that the non-perturbed MC simulation data equaled the experimental data at the resting state.

The reconstruction of μ_a was done by minimizing the sum of squared difference in the intensity change between the model data and the experimental data sets. The difference is given by

$$E = \sum_{Src, Det} (A_{MC}(Src, Det) - A_{EXP}(Src, Det))^2 \quad (4)$$

where A_{MC} and A_{EXP} are the MC and experimental signal intensity changes for the different source-detector pairs. The sum can be calculated over all source-detector pairs, but it may be beneficial to only use selected pairs. A central problem in optical activation imaging is how to separate the changes in the blood flow of the skin layer from the changes in the brain. In our pilot study, we selected those source-detector pairs which produced a statistically significant correlation between the time course of the oxyhemoglobin concentration and a prototype hemodynamic response time course. In the future, we want to use all pairs for imaging but this requires further experimentation and modelling.

The minimization was done using a simple steepest descent method.

2) *Simulated case*: In the simulated case, a brain activation was simulated by an inclusion with higher μ_a within the gray matter. A strong 50% increase in μ_a was used. MC simulations with and without the inclusion were performed to produce the simulated brain activation and resting state data.

III. RESULTS

A. Simulated data

Producing the photon biographies needed in pMC took five hours per light source position on a 64-bit AMD Opteron processor. The reconstruction itself could be performed in

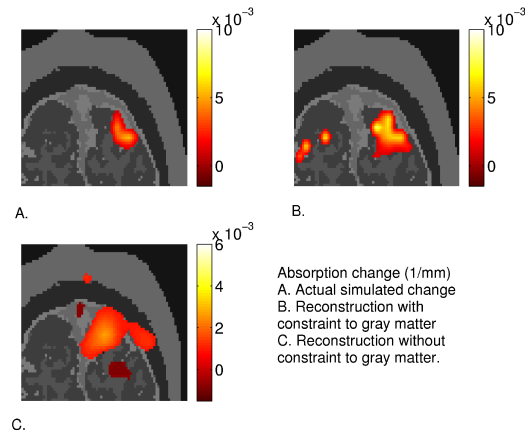


Fig. 3. pMC reconstruction of change in μ_a . Figures A, B and C show the actual simulated change in μ_a , and reconstructions obtained with and without restriction to gray matter. Due to difference in resolution between anatomical data and reconstruction of change in μ_a , some of the reconstructed μ_a change appears outside gray matter regions also in the constrained case, when superimposed in 2D.

less than 30 seconds once the photon biography data was available.

The reconstruction of μ_a was carried out both without constraints and by restricting the change in μ_a to the gray matter. The part of the head under the optical fiber array was subdivided into cubical subregions with 3 mm side length, and the value of μ_a was allowed to change independently in each subregion. Only those subregions which were probed by a significant number of detected photon packets were considered in the reconstruction. For the unconstrained case, this yielded approximately 9000 independent regions, and with restriction to gray matter, approximately 4000 independent parameters to be estimated in the reconstruction. Figure 3 shows the actual change in μ_a and slices of the reconstructed images obtained with and without restriction to the gray matter of the brain.

The results show that pMC can be used for localising absorption changes within tissue. When change in μ_a was constrained to the gray matter, the region with strongest absorption change was correctly identified. Other, weaker absorption changes are also seen in the reconstruction. The additional areas are partly due to statistical noise in the simulation and the fact that the number of source-detector pairs used in the study are not sufficient to guarantee a unique result in this geometry. In the unconstrained reconstruction, the site of strongest absorption change is correctly identified, but the large change in μ_a in a small region is reconstructed as a smaller μ_a change in a larger region.

B. Topographic maps of measured data

Topographic maps of the haemodynamic response were made using the MBLL and interpolation. Figure 4 illustrates the average change in oxyhaemoglobin concentration between the resting state and 5 s after the onset of the stimulation. The optical fiber array is shown superimposed on the data. Crosses and circles represent sources and detectors, respectively.

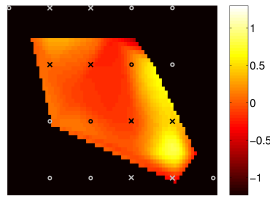


Fig. 4. Topographic map of the oxyhaemoglobin concentration change (micromolars) due to brain activation (5 s after stimulus).

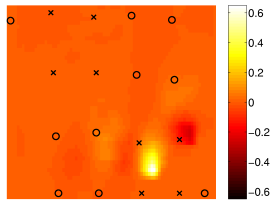


Fig. 5. Map of oxyhaemoglobin concentration change (micromolars) due to brain activation (5 s after stimulus) reconstructed using pMC.

The topographic picture shows the strongest haemodynamic change in the lower right quadrant on the fiber array. The increase in oxyhaemoglobin concentration and simultaneous decrease in deoxyhaemoglobin indicates increased blood flow. As a subset of the source-detector pairs were used to generate this image, the regions outside these pairs are displayed in black.

C. pMC reconstruction of measured data

The distribution of the absorption change was iteratively solved for using experimental data in the same manner as in the simulated case. The data from the measurements at the two wavelengths (760 nm and 830 nm) were used to reconstruct 3D maps of the change in μ_a at these wavelengths. The change in μ_a was not constrained to gray matter. The 3D map of the change in the concentration of oxyhaemoglobin was calculated from the changes in μ_a for the two wavelengths with the assumption that the change in μ_a was due to changes in oxy- and deoxyhaemoglobin. The specific extinction coefficients for these chromophores and the wavelengths used were obtained from literature [10].

In Figure 5, a 2D slice of the reconstructed 3D map of oxyhaemoglobin concentration change is shown. The slice is taken at depth of approximately 2 cm. The reconstruction shows the strongest oxyhaemoglobin concentration change at this depth, and it also coincides approximately with the surface of the brain. Locations of the source and detector fibers, projected on the slice, are shown to facilitate comparison with the topographic image.

In the reconstruction, the the strongest oxyhaemoglobin concentration change is found in the lower right quadrant of the fiber array. The result is similar to the topographic picture.

IV. CONCLUSION

We have presented a pMC method that can be used for studying optical measurements of haemodynamic changes in

the brain. The reconstructions done from simulated activation data and from experimental data indicate that pMC can be useful in localising absorption changes.

As the sensitivity of optical imaging is much greater to physiological phenomena in the skin than changes in the brain, it is necessary to develop methods for the identification of these processes. Two approaches can be used: temporal correlation of the optical data with separate measurements of global physiology, such as the heart rate, the blood pressure, and respiration may allow the suppression of those components in the optical measurements of the head. Increased numbers of sources and detectors on the surface of the head may allow the spatial separation of the skin from the brain, using appropriate modeling and reconstruction methods. Finally, these temporal and spatial identification methods can be combined. On a positive note, the skin component in neonates is of less importance than in the adult head.

V. ACKNOWLEDGMENTS

The authors would like to thank the Finnish Cultural foundation, the Finnish Academy of Science and Letters the Finnish Foundation for the advancement of Technology for financial support. The use of computing facilities of the Bioinformatics Unit of Biomedicum Helsinki is gratefully acknowledged. J.H. would like to acknowledge funding from special governmental grant for health sciences research TYH 4212.

REFERENCES

- [1] D. A. Boas, J. P. Culver, J. J. Stott and A. K. Dunn, "Three dimensional Monte Carlo code for photon migration through complex heterogenous media including the adult human head," *Opt. Express*, **10**, 159-170 (2002).
- [2] I. Nissilä, T. Noponen, K. Kotilahti, and T. Katila, L. Lipiäinen, T. Tarvainen, M. Schweiger and S. Arridge, "Instrumentation and calibration methods for the multichannel measurement of phase and amplitude in optical tomography," *Rev. Sci. Instrum.* **76**, 044302 (2005)
- [3] Polhemus Inc., 40 Hercules Drive, P.O. Box 560, Colchester, VT 05446, USA
- [4] J. Heiskala, I. Nissilä, T. Neuvonen, S. Järvenpää, E. Somersalo, "Modeling anisotropic light propagation in a realistic model of the human head," *Appl. Opt.* **44**, 11 (2005)
- [5] S. A. Prahl, M. Keijzer, S. L. Jacques, and A. J. Welch, "A Monte Carlo model of light propagation in tissue," in *Dosimetry of Laser Radiation in Medicine and Biology*, G. J. Müller and D. H. Sliney, eds., SPIE IS **5**, 102-111 (1989)
- [6] L. Wang, S. L. Jacques and L. Zheng, "MCML-Monte Carlo modeling of light transport in multi-layered tissues," *Computer Methods and Programs in Biomedicine*, **47**, 131-146 (1995)
- [7] C. Hayakawa, J. Spanier, F. Bevilacqua, A. Dunn, J. You, B. Tromberg, V. Venugopalan, "Perturbation Monte Carlo methods to solve inverse photon migration problems in heterogeneous tissues," *Opt. Lett.* **26** (2001)
- [8] J. Spanier and E. M. Gelbardm, *Monte Carlo Principles and Neutron Transport Problems* (Addison-Wesley, Reading Mass., 1969)
- [9] Y. Phaneendra Kumar, R. M. Vasu, "Reconstruction of optical properties of low-scattering tissue using derivative estimated through perturbation Monte-Carlo method, *Journal of Biomedical Optics* **9** (2004)
- [10] M. Cope, "Application of near infrared spectroscopy to non invasive monitoring of cerebral oxygenation in the newborn infant," PhD Thesis, Department of Medical Physics and Bioengineering, University College London (1991)